Target Fast Reconstruction of Real Aperture Radar Using Data Extrapolation-Based Parallel Iterative Adaptive Approach

Deqing Mao, *Student Member, IEEE*, Yongchao Zhang, *Member, IEEE*, Yin Zhang, *Member, IEEE*, Weibo Huo, *Member, IEEE*, Jifang Pei, *Member, IEEE*, and Yulin Huang, *Senior Member, IEEE*

***Abstract*—Real aperture radar (RAR) usually sweeps a wide sector to continuously observe the scenario of interest. Because its angular resolution is limited by the size of the antenna aperture, target reconstruction methods are widely applied to obtain super-resolution radar images. However, the wide-sector processing mode suffers from high operational complexity because of the high-dimensional matrix inversion. Even worse, for the targets located at the scene edge, its echo data are received less than half beamwidth. The incomplete echo data will lead to the deformation of the reconstructed targets by existing reconstruction methods. To overcome the two problems, a data extrapolation-based parallel iterative adaptive approach is proposed to fast reconstruct the targets in the whole sector without the distortion at the scene edge. First, the echo model of RAR is repaired to remedy the model error. Then, based on the correlation of the echo data within one beamwidth, an autoregressive model is adopted to extrapolate the data of the missing half beamwidth. Finally, a parallel iterative adaptive approach method is proposed to efficiently recover the targets by exploiting the regular characteristics of the repaired steering matrix. Simulations and experimental data are applied to verify the proposed method.**

***Index Terms*—Parallel iterative adaptive approach (PIAA), real aperture radar (RAR), scene edge target reconstruction, super-resolution imaging.**

I. Introduction

REAL aperture radar (RAR) usually works in scanning mode to measure the region of interest [1]. In applications of airborne radar, shipboard radar, weather radar, and so on, its antenna aperture is limited by the platforms, which leads to coarse angular resolution. Target reconstruction methods are effective to improve the angular resolution of RAR [2]–[5]. However, these methods are usually time-consuming because the target reconstruction requires high-dimensional matrix inversion. Even worse, for the targets who are located within the half-beam width of scene edge, their echo data are incompletely received [6]. When the targets are reconstructed using the incomplete echo data, the distortion phenomenon will appear for the scene edge targets [7]–[9].

To accurately and efficiently reconstruct the targets of the whole observation sector, the accurate echo model, the complete echo data, and fast inversion processing are indispensable [6], [10]. The echo model of RAR can be established in the time domain and frequency domain [11]–[14]. In the time domain, the echo data of RAR can be expressed as a convolution relationship between the antenna pattern and targets [15]–[17]. In [18], a sparse Bayesian super-resolution method is proposed to improve the angular resolution. The method utilizes the Laplace prior of targets' statistical distribution to obtain a sparse imaging result. However, the sparse method is sensitive to the noise. In [13], a truncated singular value distribution (TSVD)-based strategy is proposed to reduce the influence of noise. However, the improvement of the angular resolution is limited. Regretfully, the methods mentioned above adopt a truncated steering matrix because they ignore the model error of the scene edge targets [19]. In [6], the authors propose a TSVD with least-squares optimization (LSTSVD) method using a repaired steering matrix to well model the echo data. The repaired steering matrix can illustrate the scanning process of antenna when it sweeps the scene edge targets. However, even the model error is remedied, the echo data of scene edge targets are incomplete because they are radiated by half-beam width. The incomplete echo data will lead to a performance loss of angular super-resolution. In the frequency domain, the target reconstruction problem can be transformed into a linear inverse filtering problem. The Wiener filtering method is a traditional method to improve image quality from the frequency domain [20], [21]. However, the resolution performance of the method is limited under low echo signal-to-noise (SNR) ratio. To overcome the deficiency of Wiener filtering, a nonparametric, iterative adaptive, weighted least square-based method [spectral iterative adaptive approach (IAA)] is proposed [22]. Furthermore, to fast reconstruct the target, a wideband sparse reconstruction method is proposed based on a generalized sparse iterative covariance-based estimation algorithm [23]. However, these frequency-domain methods rely on a strict convolution model between the target and antenna pattern. For the scene edge targets, the model and methods in

Manuscript received September 30, 2020; revised November 25, 2020 and December 24, 2020; accepted January 20, 2021. Date of publication January 25, 2021; date of current version February 11, 2021. This work was supported in part by the National Natural Science Foundation of China under Grant 61901092, Grant 61901090, and Grant 61671117. *(Corresponding author: Yongchao Zhang.)*

The authors are with the School of Information and Communication Engineering, University of Electronic Science and Technology of China, Chengdu 611731, China (e-mail: mdq_uestc@163.com; zhang_yongchao1@163.com; yinzhang@uestc.edu.cn; hwbuyi@163.com; peijfstudy@126.com; yulinhuang@uestc.edu.cn).

Digital Object Identifier 10.1109/JSTARS.2021.3054046

This work is licensed under a Creative Commons Attribution 4.0 License. For more information, see https://creativecommons.org/licenses/by/4.0/

the frequency domain exist unacceptable errors as the simulation results show.

Many approaches are researched to solve the incomplete echo data problem [24]–[28]. In [24], the nonuniform sampling model is proposed to describe the incomplete echo data case. However, for the scene edge targets, the nonuniform sampling model cannot be applied because half-beam width echo data are missed. In another way, the incomplete data can be predicted by data extrapolation method [26], [27], [29], [30]. In [26], the authors propose a knowledge-aided Doppler beam sharpening (DBS) imaging method to extrapolate the azimuthal echo data. The method extrapolates the echo data by introducing the autoregressive (AR) model. However, in DBS imaging technology, the predicted echo data should keep a strict phase relationship. In [27], based on a multi-input and dual-output radar configuration, the AR model is introduced to fuse the echo data of two transmitters, which can improve the imaging resolution for radar array signal processing. However, because the imaging mechanisms of these systems are different, the echo characteristics are differently modeled.

The truncated steering matrix mentioned above presents Toeplitz structure, which can be exploited to reduce the operational complexity in inversion processing [31]. In [32], [33], the authors proposed an online Tikhonov method to fast reconstruct the targets. However, these methods not only suffer from noise amplification in such an ill-posed problem, but also cannot be fast implemented using the repaired steering matrix. Based on the accurate echo model and complete echo data, in [34], [35], the IAA method presents an excellent noise suppression performance. However, the method is time-consuming because its wide-sector processing mode requires high-dimensional matrix inversion. Furthermore, a fast IAA (FIAA) using the block tridiagonal structure of the echo autocorrelation matrix is proposed [12]. The method presents a superior angular super-resolution performance with low operational complexity, but the fixed number of iterations for each range bin is redundant. In [36], a range-recursive IAA (IAA-RR) is proposed to accelerate iterative convergence of the IAA method relying on the echo correlation of adjacent range bins. However, due to the successive implementation structure, its operational complexity increases with the increase of the number of azimuthal sampling points.

In this article, to fast reconstruct the targets of the whole observation sector, a data extrapolation-based IAA (DE-PIAA) is proposed. First, to well model the scanning process of the radar antenna, the steering matrix is repaired to remedy the model error. Then, based on the correlation of the echo data within one beamwidth, the AR model is adopted to extrapolate the missing half-beam data for the scene edge targets. Finally, based on the circle structure of the repaired steering matrix, a parallel IAA (PIAA) is proposed to recover the targets efficiently. Based on the proposed PIAA method, the operational complexity is independent of the dimensions of the observation region, and the operational efficiency can be greatly improved.

The rest of this article is organized as follows. In Section II, the echo model of RAR is introduced, and the problems of existing target reconstruction methods are analyzed. In Section III, the proposed DE-PIAA method is detailed. In Sections IV and V, simulations and experimental data are given to verify the proposed method. The conclusions is given in Section VI.

II. Related Work Review

A. Echo Signal Model

As shown in Fig. 1, a radar beam sweeps the range from $-\theta_0 \sim +\theta_0$ with an angular velocity ω. After echo preprocessing, the echo profile of the mth range bin can be described as the convolution relationship between the target scattering coefficients and the antenna pattern [12], which can be modeled as

$$\boldsymbol{y}_m = \mathbf{A}\boldsymbol{\sigma}_m + \mathbf{e}_m \tag{1}$$

where $\boldsymbol{y}_m \in \mathbb{C}^{N\times 1}$, $\boldsymbol{\sigma}_m \in \mathbb{C}^{N\times 1}$, and $\mathbf{e}_m \in \mathbb{C}^{N\times 1}$ represent echo data, target scattering coefficients, and additive white noise of the mth range bin, respectively. The steering matrix $\mathbf{A} = (\boldsymbol{a}_1, \boldsymbol{a}_2, \ldots, \boldsymbol{a}_N) \in \mathbb{C}^{N\times N}$ can be established by the antenna pattern $\boldsymbol{h} = [a(\theta_1), a(\theta_2), \ldots, a(\theta_L)]$ as

$$\mathbf{A} = \begin{bmatrix} a(\theta_{L/2}) & \cdots & a(\theta_1) & & & & \\ \vdots & \ddots & \vdots & \ddots & & & \\ a(\theta_L) & \vdots & \ddots & \vdots & a(\theta_1) & & \\ & a(\theta_L) & \vdots & \ddots & \vdots & \ddots & \\ & & a(\theta_L) & \vdots & \ddots & \vdots & a(\theta_1) \\ & & & \ddots & \vdots & \ddots & \vdots \\ & & & & a(\theta_L) & \cdots & a(\theta_{L/2}) \end{bmatrix} \tag{2}$$

where $L = \theta_\beta * \mathrm{PRF}/\omega$. θ_β and PRF denote the beam width and pulse repetition frequency, respectively. N denotes the number of sampling points in the azimuthal direction. Clearly, the steering matrix is truncated because the scanning beam stops at the scene edge. The echo data of the targets located at scene edge are incompletely received.

B. Problem Analysis

Based on the echo model above, we cannot well reconstruct the targets in the whole observation range. On the one hand, because of the model error and incomplete echo data, the distortion of scene edge targets appears. On the other hand, the Toeplitz structure of the truncated steering matrix is destroyed, which leads to the operational burden of matrix inversion.

The model error refers to the truncation of the steering matrix in (2). As shown in Fig. 1, when the radar beam center radiates the target T2, half of the beam width is radiated out of the scanning scene. As illustrated by target T1, if a target exists outside of the observation range, its echo data are still received in advance. The truncated steering matrix cannot be applied to accurately describe the radiation relationship between the targets and the radar beam. To remedy the model error, the echo model can be transformed into

$$\boldsymbol{y}_m = \mathbf{A}'\boldsymbol{\sigma}'_m + \mathbf{e}_m \tag{3}$$

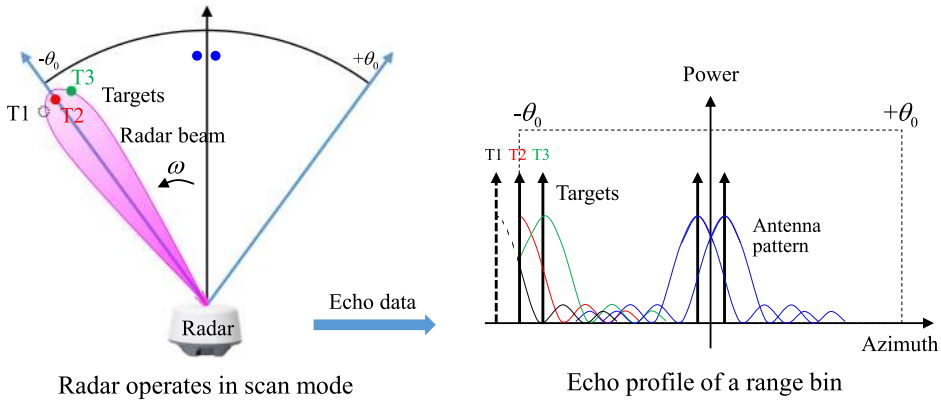

Fig. 1. Operating mode and echo profile of real aperture scanning radar.

where the repaired steering matrix $\mathbf{A}' = (\boldsymbol{a}'_1, \boldsymbol{a}'_2, \ldots, \boldsymbol{a}'_K) \in \mathbb{C}^{N\times K}$ can be established by the antenna pattern and the dimension of the echo data as

$$\mathbf{A}' = \begin{bmatrix} a(\theta_1) & a(\theta_2) & \cdots & a(\theta_L) & & \\ & a(\theta_1) & a(\theta_2) & \cdots & a(\theta_L) & \\ & & \ddots & \ddots & \ddots & \ddots \\ & & & a(\theta_1) & a(\theta_2) & \cdots & a(\theta_L) \end{bmatrix}. \quad (4)$$

Based on the convolution theory of echo data, the determined relationship among N, L, and K can be represented as $K = L + N - 1$. The target scattering coefficients $\boldsymbol{\sigma}'_m$ can be expressed as

$$\boldsymbol{\sigma}'_m = [\boldsymbol{\sigma}'_l, \boldsymbol{\sigma}_m, \boldsymbol{\sigma}'_r]^T \quad (5)$$

where $\boldsymbol{\sigma}'_l$ and $\boldsymbol{\sigma}'_r$ denote the reconstructed targets that are outside the observation range but within half beam width of the left and right parts, respectively. T represents the transpose operation. Based on the remedied echo model in (3), the repaired steering matrix can be applied to accurately describe the acquisition process of echo data.

In addition, the echo data of the scene edge targets are incompletely received. Although the model error is remedied as above, the echo data of the scene edge targets are received less than one beamwidth. For example, the echo data of target T3 are received by $3/4$ beamwidth, and that of the target T2 are received by half beamwidth. The incomplete echo data lead to the loss of the observed information, which deforms the reconstructed scene edge targets.

As shown in (4), the increased dimensions of the repaired steering matrix lead to extra operational burden. Meanwhile, the Toeplitz structure of the truncated steering matrix is destroyed. As a result, some traditional acceleration methods in [32]–[31] cannot be applied to reduce the notably high computational complexity. The targets are difficult to be fast reconstructed based on the high-dimensional echo data.

III. Proposed Method

In this article, to solve the problems as above, we propose a DE-PIAA method to reconstruct the targets in parallel. First, based on the correlation of the echo data within one beamwidth, we extrapolate the echo data of the scene edge targets using the AR model. Then, the repaired steering matrix is adopted to model the scanning process of radar antenna. Finally, using the independent relationship of the echo data from adjacent beamwidths, we propose a PIAA method to fast reconstruct the targets. The schematic of the proposed DE-PIAA method is shown in Fig. 2.

A. Data Extrapolation

As the repaired echo model shown in (3), the echo data of the mth range bin can be expressed as

$$\boldsymbol{y}_m = [y_1, \ldots, y_n, \ldots, y_N]^T. \quad (6)$$

The echo data within the observation range are correlated with the missing half beamwidth data. To extrapolate the data of the left direction (backward direction), the Yule–Walker equation can be expressed as

$$\mathbf{R}_L \begin{bmatrix} 1 \\ \lambda_1 \\ \vdots \\ \lambda_P \end{bmatrix} = \begin{bmatrix} \delta^2 \\ 0 \\ \vdots \\ 0 \end{bmatrix} \quad (7)$$

where $\mathbf{R}_L$ denotes the echo autocorrelation matrix of the left part echo data. $\boldsymbol{\lambda} = (\lambda_1, \ldots, \lambda_p, \ldots, \lambda_P)^T$ is the P order AR coefficients. δ^2 represents the noise variance. Based on the Hermitian structure of the echo autocorrelation matrix, the AR coefficients can be fast solved according to the LDL-factorization algorithm [37].

Based on the AR coefficients, the extrapolated echo data can be expressed as

$$y'_1 = \sum_{p=1}^{P} \lambda_p y_p \quad (8)$$

where y'_1 represents the first extrapolated point. Based on the sequence of echo points, the extrapolated data of backward direction can be obtained by a recursive process. Meanwhile, to obtain the extrapolated data of the right direction (forward direction), the AR coefficients can be solved based on the Yule–Walker equation of the right part data.

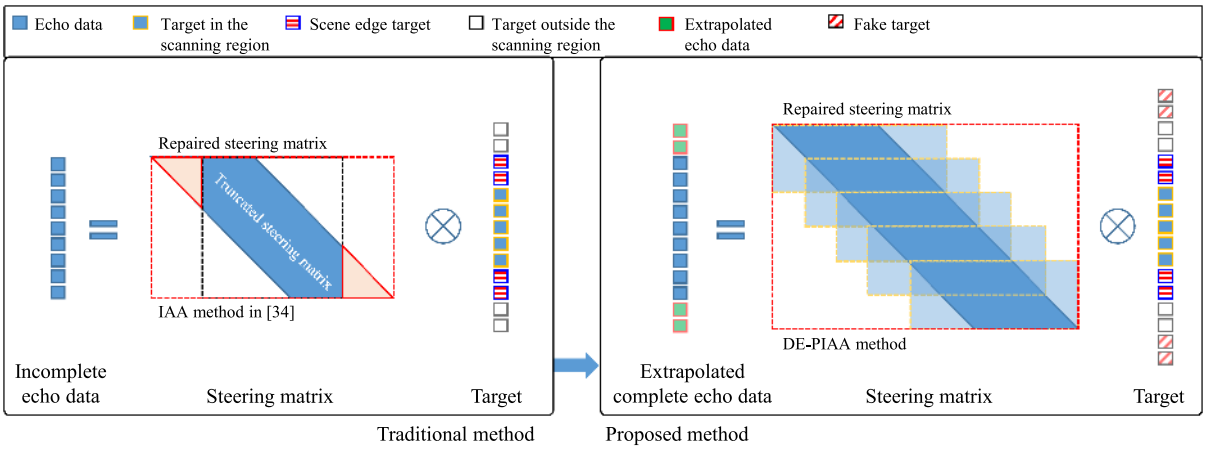

Fig. 2. Process diagram.

Then, the completed echo data can be expressed as

$$\boldsymbol{y}'_m = [y'_{L/2}, \ldots, y'_1; y_1, \ldots, y_n, \ldots, y_N; y''_1, \ldots, y''_{L/2}]^T \quad (9)$$

where $(y'_{L/2}, \ldots, y'_1)^T$ and $(y''_1, \ldots, y''_{L/2})^T$ represent the extrapolated data of backward direction and forward direction, respectively. Clearly, the echo data of the scene edge targets become complete using the data extrapolation process. As shown in the right part of Fig. 2, the scene edge targets can be reconstructed based on the extrapolated complete echo data.

It is noted that the repaired steering matrix is an underdetermined matrix, which makes the dimension of the reconstructed targets larger than that of the echo data. However, based on the targets' direction information, the reconstructed targets outside of the observation range and the fake targets, as shown in Fig. 2, will be ignored.

B. Proposed PIAA Method

Based on the process of data extrapolation, the echo data of the scene edge targets become complete. As shown in Fig. 2, the repaired steering matrix presents a circular structure along the row direction. Using the circular structure, we propose a PIAA method to reconstruct the targets efficiently. The operational complexity is analyzed in detail.

1) Proposed PIAA Method: Using the complete echo data shown in (9), the repaired steering matrix should be reconstructed as a $K \times (K + L - 1)$ matrix. As shown in Fig. 2, the repaired steering matrix $\mathbf{A}''$ can be expressed as

$$\mathbf{A}'' = (\boldsymbol{a}''_1, \ldots, \boldsymbol{a}''_i, \ldots, \boldsymbol{a}''_{L+K-1})^T \quad (10)$$

where $\boldsymbol{a}''_i$ denotes the steering vector of the ith direction. It is seen that the dimension of the repaired steering matrix is increased. Because the target reconstruction relies on an inversion process of the repaired steering matrix, the computational complexity of the matrix inversion operation is high. From the structure of the repaired steering matrix, we find that the inversion process can be achieved in parallel because the echo data of different beams are independent. Although the dimension of the repaired steering matrix is large, its inversion process can be divided into the inversion of several small matrices, as illustrated in the right part of Fig. 2.

To reconstruct the targets based on the complete echo data in (9), the echo data within two beamwidths are recursively divided into coherent processing intervals (CPIs). The echo data can be transformed into

$$\boldsymbol{y}'_{\mathrm{m}} = \overbrace{[y'_{\mathrm{L/2}}, \ldots, y'_1; y_1, \ldots, y_{\mathrm{L/2}}, \ldots, y_{3\mathrm{L/2}}}^{\text{CPI 1}}, \cdots, \overbrace{y_{5\mathrm{L/2}}}^{\text{CPI 2}}, \cdots y_{\mathrm{n}}, \ldots, y_{\mathrm{N}}; y''_1, \ldots, y''_{\mathrm{L/2}}]^{\mathrm{T}} \quad (11)$$

It is seen that the echo data of every two beamwidths are independent. Therefore, they can be processed in parallel.

To fast reconstruct the targets, for the data of each CPI, the proposed PIAA method can be illustrated as

$$\hat{\sigma}^{(\kappa)}(\theta_\eta) = \frac{\boldsymbol{a}'^H_\eta [\mathbf{R}^{(\kappa)}]^{-1} \boldsymbol{y}_{1:2\,L}}{\boldsymbol{a}'^H_\eta [\mathbf{R}^{(\kappa)}]^{-1} \boldsymbol{a}'_\eta} \quad (12)$$

$$\mathbf{R}^{(\kappa+1)} = \sum_{\eta=1}^{3\,L} \hat{\sigma}^{2(\kappa)}(\theta_\eta) \boldsymbol{a}'_\eta \boldsymbol{a}'^H_\eta = \mathbf{A}'_1 \mathbf{P}' \mathbf{A}'^H_1 \quad (13)$$

where $\eta = 1, \ldots, 3\,L$ represents the number of the reconstructed targets. κ denotes the number of iterations. H represents the conjugate transposition operation. $\boldsymbol{y}_{1:2\,L}$ denotes the azimuthal echo data of one CPI. $\hat{\sigma}^{(\kappa)}(\theta_\eta)$ is the target scattering coefficient of ηth direction in the κth iteration. $\mathbf{R}^{(\kappa)}$ is the echo autocorrelation matrix in the κth iteration. $\mathbf{A}'_1 = [\boldsymbol{a}'_1, \ldots, \boldsymbol{a}'_\eta, \ldots, \boldsymbol{a}'_{3\,L}] \in \mathbb{C}^{2\,L \times 3\,L}$, and $\mathbf{P}' = diag(\hat{\sigma}^{2(\kappa)}(\theta_1), \ldots, \hat{\sigma}^{2(\kappa)}(\theta_\eta), \ldots, \hat{\sigma}^{2(\kappa)}(\theta_{3\,L}))$ is a diagonal matrix. It is obvious that the operational dimension of the data is significantly reduced. The echo autocorrelation matrix can be initialized by the identity matrix.

For the whole range bins of the imaging scene, the data can be applied to estimate the echo autocorrelation matrix together. The reconstruction process can be transformed as

$$\hat{\boldsymbol{\sigma}}^{(\kappa)}(\theta_\eta) = \frac{\boldsymbol{a'}_\eta^H [\mathbf{R}'^{(\kappa)}]^{-1} \mathbf{Y}'_{1:2\,L}}{\boldsymbol{a'}_\eta^H [\mathbf{R}'^{(\kappa)}]^{-1} \boldsymbol{a'}_\eta} \tag{14}$$

$$\boldsymbol{\gamma}^{(\kappa)} = \frac{1}{M} \sum_{m=1}^{M} \left| \hat{\boldsymbol{\sigma}}_m^{(\kappa)} \right|^2 \tag{15}$$

$$\begin{aligned} \mathbf{R}'^{(\kappa+1)} &= \sum_{\eta=1}^{3\,L} \boldsymbol{\gamma}^{(\kappa)}(\theta_\eta) \boldsymbol{a'}_\eta \boldsymbol{a'}_\eta^H \\ &= \mathbf{A}'_1 \mathbf{P}'' \mathbf{A}_1'^H \end{aligned} \tag{16}$$

where $\mathbf{Y}'_{1:2\,L} \in \mathbb{C}^{2L \times M}$ denotes the echo data of the whole range bins for one CPI. $\boldsymbol{\gamma}^{(i)} = [\gamma^{(i)}(\theta_1), \boldsymbol{\gamma}^{(i)}(\theta_2), \ldots, \boldsymbol{\gamma}^{(i)}(\theta_{3\,L})]^T$ denotes the average signal power of the scattering coefficients, and $\mathbf{P}'' = diag(\gamma^{(\kappa)}(\theta_1), \gamma^{(\kappa)}(\theta_2), \ldots, \gamma^{(\kappa)}(\theta_{3\,L}))$. M denotes the number of the range sampling points.

To avoid the noise amplification caused by underdetermined matrix inversion, we repair the echo autocorrelation matrix by introducing a diagonal loading as

$$\mathbf{R}''^{(\kappa)} = \mathbf{R}'^{(\kappa)} + \alpha \mathbf{I} \tag{17}$$

where α is a penalty item, and $\mathbf{I}$ denotes a identity matrix [38]. Finally, the reconstructed targets' scattering coefficients can be combined according to their direction information.

2) Fast Implementation of the PIAA Method: It is seen that the above PIAA method mainly consists of three steps. The operational complexity lies in the calculation of the autocorrelation matrix and its inversion. To further improve its operational efficiency, the autocorrelation matrix and its inversion can be efficiently obtained based on the circle structure of the repaired steering matrix.

On the one hand, as shown in (16), the echo autocorrelation matrix can be expressed by twice convolution operations based on the relationship between the antenna pattern $\boldsymbol{h}$ and the targets' power matrix $\mathbf{P}''$. The echo autocorrelation matrix can be expressed as

$$\mathbf{R} = \left[\boldsymbol{h} \otimes [\boldsymbol{h} \otimes \mathbf{P}'']_{L:3\,L-1}^H \right]_{L:3\,L-1}^H \tag{18}$$

where $\otimes$ denotes the convolution operation between the antenna pattern and the column vector of $\mathbf{P}''$. $[\cdot]_{L:3\,L-1}$ represents the matrix truncation for its L to $3\,L-1$ rows. Clearly, the convolution operation can be efficiently achieved by fast Fourier transform. Therefore, the echo autocorrelation matrix can be fast calculated.

On the other hand, we find that the autocorrelation matrix presents Hermitian structure, which can be applied to achieve fast inversion. The echo autocorrelation matrix after diagonal loading can be decomposed into

$$\mathbf{R}' = \mathbf{L}\mathbf{D}\mathbf{L}^T \tag{19}$$

where $\mathbf{L}$ and $\mathbf{D}$ denote a lower triangular matrix and a diagonal matrix, respectively. $\mathbf{D} = diag(d_1, d_2, \ldots, d_{2\,L})$, and the matrix

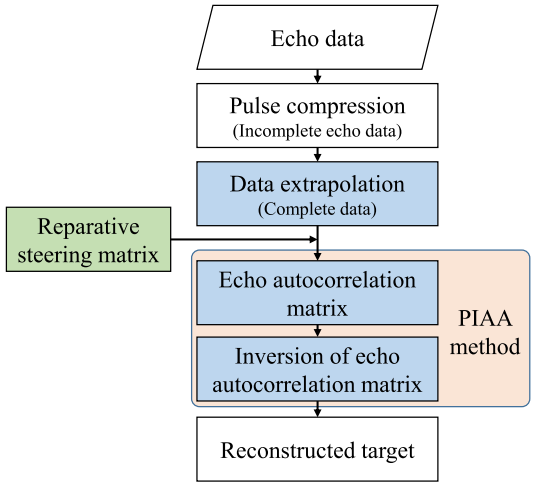

Fig. 3. Flowchart of the proposed DE-PIAA method.

$\mathbf{L}$ can be expressed as

$$\mathbf{L} = \begin{bmatrix} 1 & & & \\ l_{2\times 1} & 1 & & \\ \vdots & \ddots & \ddots & \\ l_{2\,L\times 1} & \cdots & l_{2\,L\times 2\,L-1} & 1 \end{bmatrix}. \tag{20}$$

The factorized matrix can be explicitly obtained based on the LDL-factorization algorithm [37] as

$$\begin{cases} d_j = r_{jj} - \sum_{\beta=1}^{j-1} l_{j\beta}^2 d_\beta \\ l_{ij} = \left(r_{ij} - \sum_{\beta=1}^{j-1} l_{i\beta} l_{j\beta} d_\beta \right) / d_j, i > j \end{cases} \tag{21}$$

where $i = 1, 2, \ldots, 2\,L$ and $j = 1, 2, \ldots, 2\,L$ represent the number of rows and columns of $\mathbf{L}$, respectively. β is an auxiliary variable. r_{ij} denotes the element of $\mathbf{R}'$. The inversion of $\mathbf{R}'$ can be obtained by resolving the following:

$$\mathbf{L}\mathbf{D}\mathbf{L}^T \mathbf{R}'^{-1} = \mathbf{I} \Rightarrow \begin{cases} \mathbf{L}\boldsymbol{\Gamma} = \mathbf{I} \\ \mathbf{D}\boldsymbol{\Lambda} = \boldsymbol{\Gamma} \\ \mathbf{L}^T \mathbf{R}'^{-1} = \boldsymbol{\Lambda} \end{cases} \tag{22}$$

where $\boldsymbol{\Gamma}$ and $\boldsymbol{\Lambda}$ are auxiliary variables. The inversion matrix $\mathbf{R}'^{-1}$ can be expressed as

$$\begin{cases} \boldsymbol{\Gamma}_{ab} = \mathbf{I}_{ab} - \sum_{g=1}^{a-1} \mathbf{L}_{ag} \boldsymbol{\Gamma}_{gb} \\ \boldsymbol{\Lambda}_{ab} = \boldsymbol{\Gamma}_{ab} / \mathbf{D}_{aa} \\ \mathbf{R}'^{-1}_{a'b} = \boldsymbol{\Lambda}_{a'b} - \sum_{g=a'+1}^{2\,L} \mathbf{L}_{ga'} \mathbf{R}'^{-1}_{gg} \end{cases} \tag{23}$$

where $a = 1, 2, \ldots, 2\,L$, $b = 1, 2, \ldots, 2\,L$, $a' = 2\,L, \ldots, 2, 1$, and g is an auxiliary variable. Based on the Hermitian structure of the echo autocorrelation matrix, its inversion can be fast obtained using the matrix factorization.

It is noted that the fast implementation of the PIAA method is different from that of the traditional FIAA method in [39] because the characteristics of the echo autocorrelation matrix are different. The flow chart of the proposed DE-PIAA method is illustrated in Fig. 3.

C. Operational Complexity

In this article, the proposed method consists of two steps. Traditionally, the operational complexity of the data-extrapolation process is $O(LP^3 + LP)$. When the Yule–Walker equation is solved according to an acceleration method [40], the computational complexity of the data-extrapolation process can be improved to $O(LP^3/4 + LP)$.

In addition, the reconstruction of the targets based on the super-resolution methods is an inversion process. From the echo data in (3) and the steering matrix in (4), the operational complexity of high-dimensional matrix inversion is heavy. Because the Toeplitz characteristic of the steering matrix is destroyed, the IAA method cannot be implemented with the current fast algorithms, and its operational complexity is $O(K^3)$. The high-dimensional matrix inversion is difficult to be achieved in applications. The computational complexity of IAA method in [34] is $O[\kappa(2(K+L)(N+L)^2 + 2(K+L)(N+L)M + (K+L)(N+L) + (K+L)M + (N+L)^3)]$.

The IAA-RR method in [36] can accelerate the iterative convergence of the IAA method by exploiting the echo correlation of adjacent range bins. However, the operational complexity of its successive implementation structure increases with the increase of the number of azimuthal sampling points. Its operational complexity is $O[\bar{\kappa}M(\frac{1}{2}N^2L + \frac{7}{2}NL^2 - L^3)]$ [36], and $\bar{\kappa}$ denotes the average number of iterations.

Based on the proposed PIAA method, the inversion of the high-dimensional matrix can be divided into several small matrices inversion. The proposed PIAA method can solve the inversion of the large autocorrelation matrix by processing each $2L$ echo data in parallel. The computational complexity of the PIAA method can be reduced to $O[\kappa(36\,L^2 log_2(2\,L) + 24ML^2 + 12\,L^2 + 4ML + \frac{27}{4}L^3)]$ by fast implementation. The PIAA method seems complex, but the dimensions K and N are usually much larger than L. The computational complexity of the PIAA method is reduced as the simulation result shows.

As a summary, based on the extrapolated complete data, the operational complexity of the IAA method is high. The IAA-RR method can improve its operational efficiency by solving the inversion problem recursively, and its operational complexity of the successive implementation structure increases with the increasing of the azimuthal dimensions. In this article, because the echo data of adjacent beamwidths are independent, the targets can be reconstructed in parallel based on the circle structure of the repaired steering matrix. The operational complexity of the proposed PIAA method is independent of the dimensions of the observation region, which is verified by the simulations in Fig. 6.

IV. Simulation

A. Reconstruction Performance Verification

To verify the reconstruction performance of the proposed method, the simulation parameters are listed in Table I.

The original scene and its echo data are shown in Fig. 4. In Fig. 4(a), there are four targets located in the scenario. Two targets are located at the edge of the scene. The other two targets are located at the center of the scene. As shown in Fig. 4(b), the

TABLE I
Simulation Parameters

Parameter	Value	Unit
Carrier frequency	9.3	GHz
3 dB beamwidth	3	degree
Beam width	8	degree
PRF	1000	Hz
Scanning speed	60	degree/s
Imaging region	$-20 \sim 20$	degree
Order of AR model	40	

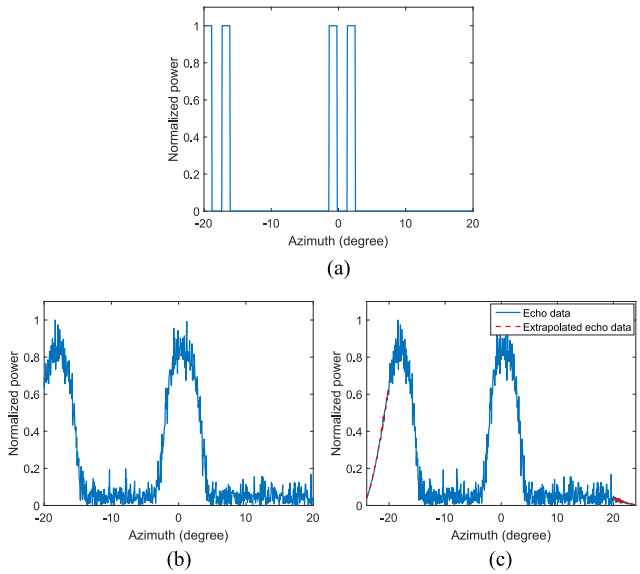

Fig. 4. Truth and echo data. (a) Truth. (b) Echo data (SNR = 15 dB). (c) Extrapolated complete echo data.

echo data of the scene edge targets are partly acquired. The echo data of the scene center targets are completely obtained. In Fig. 4(c), the echo data of the scene edge targets are extrapolated based on the proposed AR model.

Fig. 5 gives the reconstructed results by different methods of the incomplete echo data and extrapolated complete echo data. From Fig. 5(a)–(d) and (i)–(k), it is seen that the scene edge targets based on the incomplete echo data cannot be well reconstructed. To some extent, the reconstructed scene edge results based on the incomplete echo data present the target deformation phenomena. In Fig. 5(a)–(d), the scene edge targets reconstructed by the LSTSVD method, Tikhonov method and spectral IAA method, respectively, present different powers. As shown in Fig. 5(i)–(k), the powers of the reconstructed scene edge targets are lower than that of the center targets. Meanwhile, the targets' profiles of the scene edge are distorted.

Based on the data extrapolation process, the echo data of the scene edge targets become complete. In Fig. 5(e)–(f), the reconstructed performance is improved based on the extrapolated complete data. However, the sidelobe performance of the LSTSVD method is still high. The residual noise of the Tikhonov method is strong. In Fig. 5(g), the edge targets of the spectral IAA method present a certain loss because it requires a strict convolution model. As shown in Fig. 5(h), the deformation

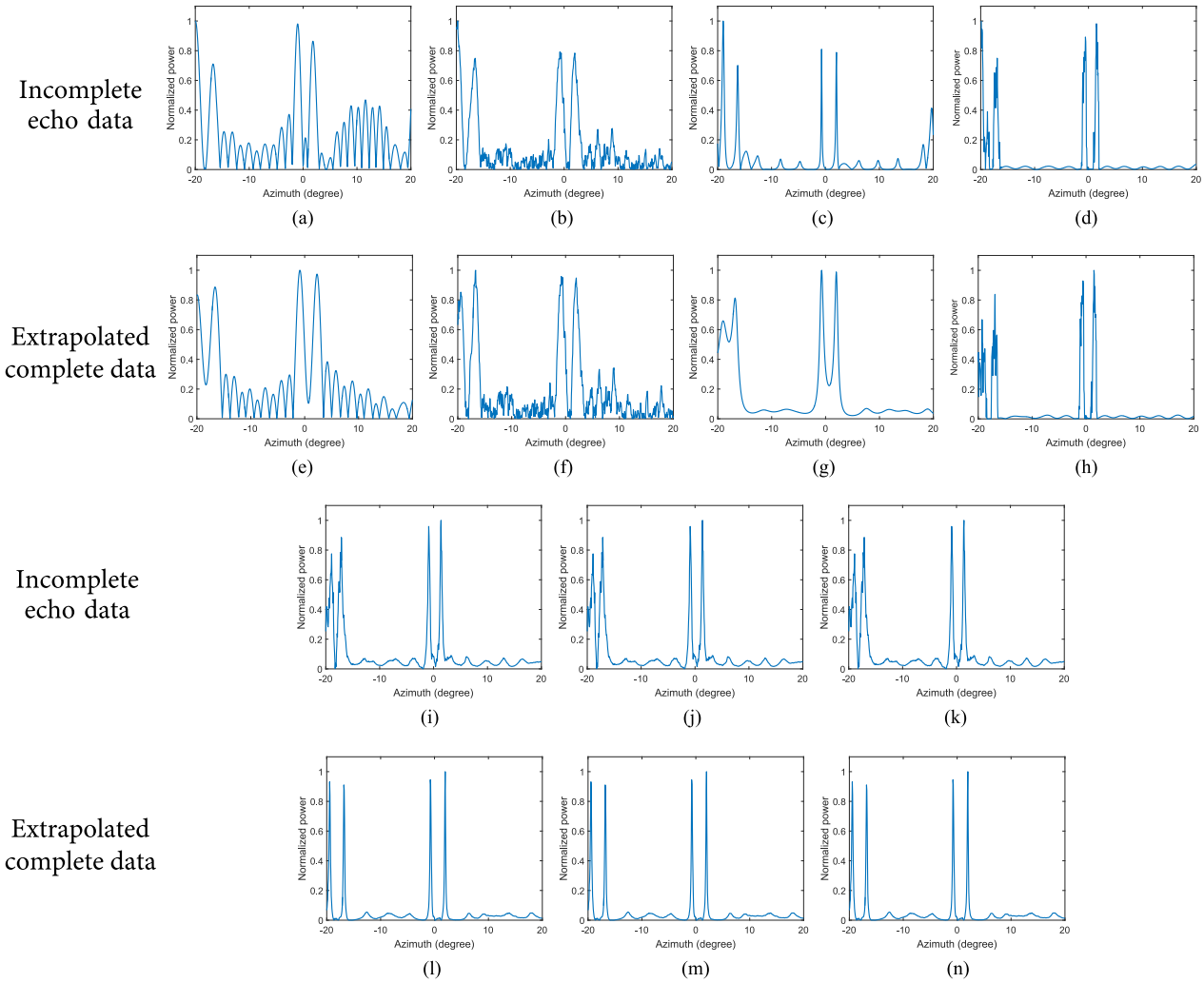

Fig. 5. Reconstructed results based on different methods. (a)–(d) Incomplete echo data. (e)–(h) Extrapolated complete echo data. (i)–(k) Incomplete echo data. (l)–(n) Extrapolated complete echo data. (a) LSTSVD method. (b) Tikhonov method. (c) Spectral IAA method. (d) Sparse Bayesian mehtod. (e) LSTSVD method. (f) Tikhonov method. (g) Spectral IAA method. (h) Sparse Bayesian mehtod. (i) IAA method. (j) IAA-RR method. (k) PIAA method. (l) IAA method. (m) IAA-RR method. (n) DE-PIAA method.

phenomena of the reconstructed edge targets are suppressed by the sparse Bayesian method. However, the targets are split because the sparse method is sensitive to noise. In Fig. 5(l)–(n), the reconstructed results of the IAA method, the IAA-RR method and the DE-PIAA method are similar. Meanwhile, the operational complexity of the DE-PIAA method is much lower.

TABLE II
SYSTEM CONFIGURATION

Platform	Configuration
CPU	Intel(R) i7-6700 CPU 3.40 GHz
RAM	16 GB
Software	Matlab R2015B

B. Performance Analysis

We proceed to compare the performance of the reconstructed results quantitatively.

1) Operational Efficiency: Based on the proposed DE-PIAA method, the operational complexity is reduced by dividing the big matrix inversion into several small matrices inversion in parallel. The proposed method is operated by the system shown in Table II. For one range bin, the operational time of different methods are compared in Fig. 6.

From Fig. 6, it is seen that the proposed method presents lower operational complexity than the traditional IAA method [34] and the IAA-RR method. When the number of data dimensions is small, e.g. $N = 256 \approx 2\,L$, the operational time of these methods is similar. However, with the increase of echo data dimensions, the operational time of the IAA method is much longer than that of the proposed method. Comparing with the IAA-RR method, the operational time of the PIAA method is independent of the number of azimuthal dimensions because it can be achieved in parallel, which can be also validated from the analysis in Section III-C. Specifically, when the dimension of the echo data is $N = 1024$, the speedup ratio of the simulated

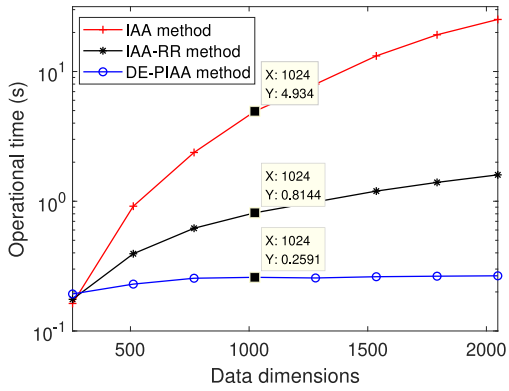

Fig. 6. Comparison of operational time.

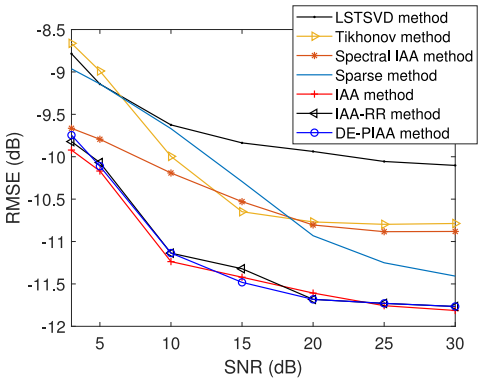

Fig. 7. Influence of echo SNR on scene edge target.

operational time respects to the IAA method is about $19\times$, while that of the IAA-RR method is $6\times$.

2) Influence of Echo SNR on Scene Edge Target: The root-mean-square error (rmse) is applied to evaluate the reconstructed performance, which is defined as

$$RMSE(\boldsymbol{\sigma}_L, \hat{\boldsymbol{\sigma}}_L) = \sqrt{\frac{1}{L}\sum_{i=1}^{L}(\sigma_i - \hat{\sigma}_i)^2} \qquad (24)$$

where $\boldsymbol{\sigma}_L$ and $\hat{\boldsymbol{\sigma}}_L$ denote the original targets and the estimated targets in one beamwidth of the scene edge. Under different echo SNRs, the rmses of different methods using the extrapolated complete data are compared in Fig. 7.

In Fig. 7, it is seen that the IAA method, the IAA-RR method and the DE-PIAA method are better than the other methods. The SNR has a limited influence on the LSTSVD method. However, the method suffers from high sidelobe performance. The Tikhonov method and sparse method are sensitive to the SNR, and these methods are difficult to be applied in low SNR circumstances. The spectral IAA method can keep a better performance in low SNR. However, with the increase of SNR, its performance improvement is limited. The rmse performance of the IAA method, the IAA-RR method and the DE-PIAA method is similar, but the DE-PIAA method presents high operational efficiency.

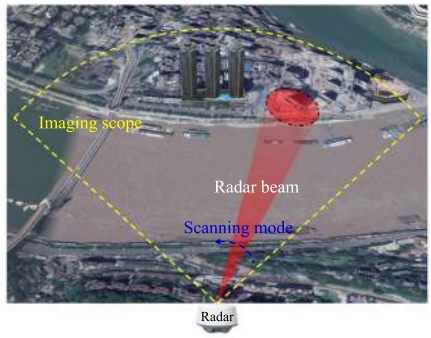

(a)

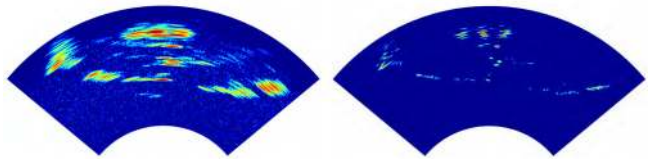

(b) (c)

Fig. 8. Experimental scenario and echo data. (a) Experimental scenario. (b) Echo data. (c) Super-resolution result.

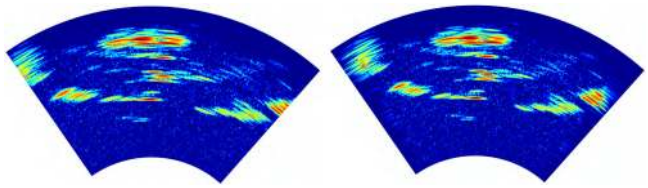

(a) (b)

Fig. 9. Comparison of the incomplete echo data and extrapolated echo data. (a) Incomplete echo data. (b) Extrapolated complete echo data.

V. Experimental Data

In the simulations, the operational efficiency of the proposed PIAA method is analyzed. In experiments, we focus on comparing the reconstruction quality of the scene edge targets. However, we cannot obtain the real target scattering coefficients in experiments. On the one hand, we first obtain a referenced reconstructed imagery based on a scene with complete echo data. The data are truncated to describe the stop of beam scanning. On the other hand, another scene with incomplete data is applied to verify the performance of the proposed method.

A. Comparison by Complete Echo Data

1) Experimental Conditions and Echo Data: As shown in Fig. 8(a), a radar scans three buildings. In Fig. 8(b), it is seen that the echo data of both scene edges are complete. Based on the complete echo data, the IAA method is adopted to obtain a referenced reconstructed imagery [34], [35], as shown in Fig. 8(c). The referenced imagery can be applied to evaluate the performance of the results reconstructed by the incomplete data.

2) Reconstructed Target Comparison of Incomplete Data: As shown in Fig. 9(a), the echo data are truncated to describe

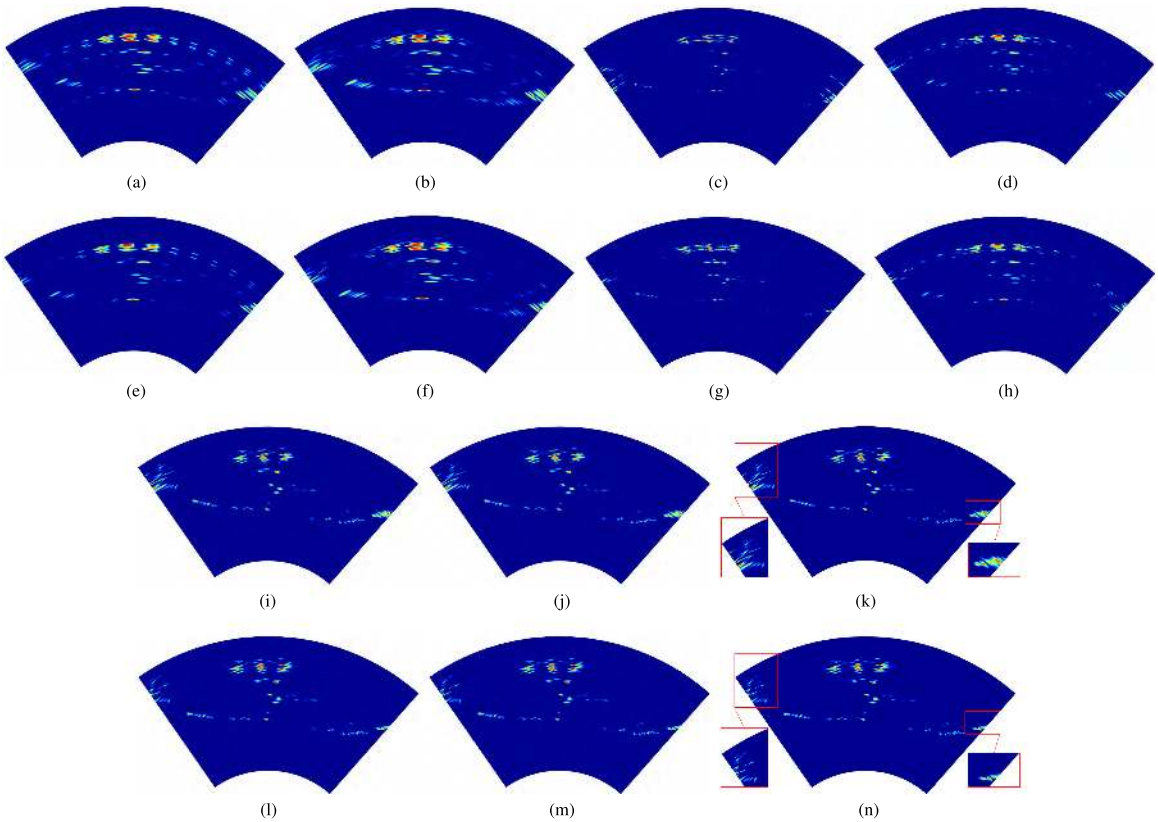

Fig. 10. Reconstructed results based on different methods. (a)–(d) Incomplete echo data. (e)–(h) Extrapolated complete echo data. (i)–(k) Incomplete echo data. (l)–(n) Extrapolated complete echo data. (a) LSTSVD method. (b) Tikhonov method. (c) Spectral IAA method. (d) Sparse Bayesian mehtod. (e) LSTSVD method. (f) Tikhonov method. (g) Spectral IAA method. (h) Sparse Bayesian mehtod. (i) IAA method. (j) IAA-RR method. (k) PIAA method. (l) IAA method. (m) IAA-RR method. (n) DE-PIAA method.

TABLE III
IMAGE CORRELATION COEFFICIENTS OF THE EDGE TARGETS

Methods	Left part	Right part
LSTSVD method	0.3364	0.2388
Tikohonov method	0.3557	0.2612
Spectral IAA method	0.5364	0.5043
Sparse Bayesian method	0.5226	0.4976
IAA method	0.8913	0.8615
IAA-RR method	0.8904	0.8607
Proposed DE-PIAA method	0.8902	0.8611

the stop of beam scanning. It is seen that the echo data of the scene edge targets are received partly. Based on the introduced data extrapolation method, the extrapolated complete echo data are shown in Fig. 9(b).

The reconstruction results using different super-resolution methods are compared in Fig. 10. It is seen that, as shown in Fig. 10(a)–(d) and (i)–(k), the constructed results based on incomplete data present performance loss for the scene targets. In Fig. 10(a), the side lobe of the LSTSVD method is high. Although the side lobe becomes lower using the Tikhonov method, the resolution improvement in Fig. 10(b) is limited. The incomplete data present a serious influence on the imaging

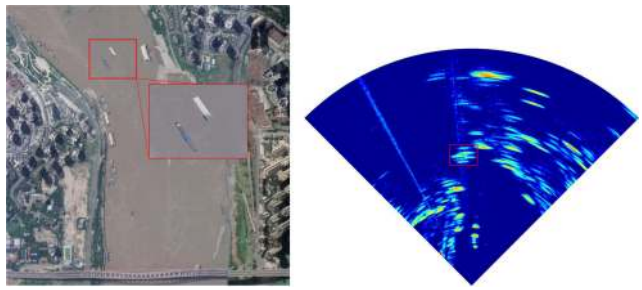

Fig. 11. Experimental scenario and incomplete echo data. (a) Experimental scenario. (b) Incomplete echo data.

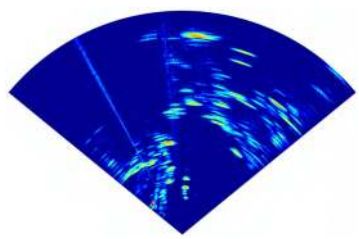

Fig. 12. Extrapolated complete echo data.

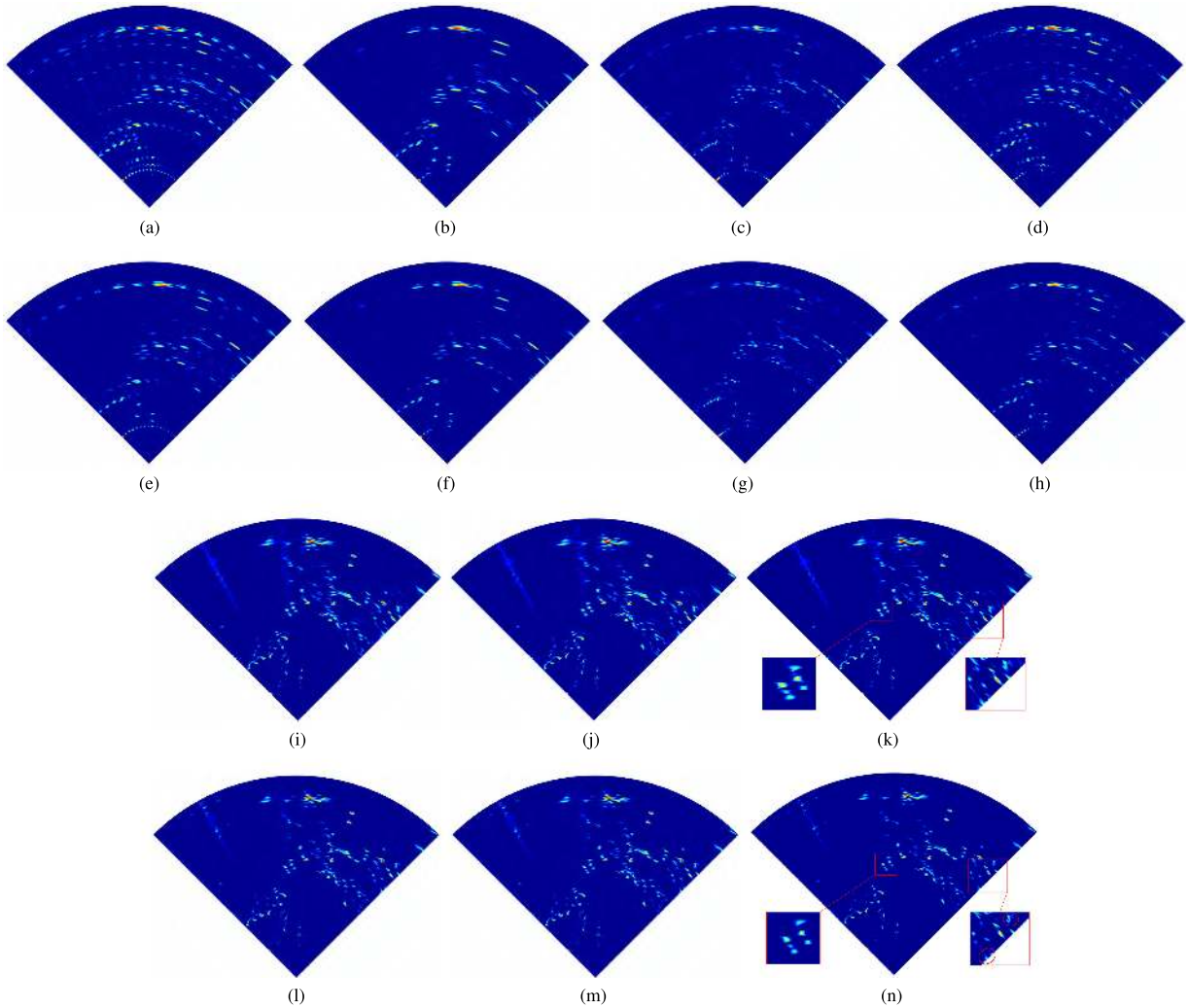

Fig. 13. Reconstructed results based on different methods. (a)–(d) Incomplete echo data. (e)–(h) Extrapolated complete echo data. (i)–(k) Incomplete echo data. (l)–(n) Extrapolated complete echo data. (a) LSTSVD method. (b) Tikhonov method. (c) Spectral IAA method. (d) Sparse Bayesian mehtod. (e) LSTSVD method. (f) Tikhonov method. (g) Spectral IAA method. (h) Sparse Bayesian mehtod. (i) IAA method. (j) IAA-RR method. (k) PIAA method. (l) IAA method. (m) IAA-RR method. (n) DE-PIAA method.

result of the spectral IAA method, as shown in Fig. 10(c). The sparse method can improve the resolution of the three buildings in Fig. 10(d), but the targets of both sides are distorted. The imaging result shown in Fig. 10(i) is superior to the other methods, however, the targets located scene edge are widened. In Fig. 10(j)–(k), the IAA-RR method and the PIAA method present similar imaging performance with the IAA method.

As shown in Fig. 10(e)–(h) and (l)–(n), the targets located at the scene edge are focused using the extrapolated complete echo data. It is seen in Fig. 10(e)–(f) that the performance of the scene center targets are kept, and the targets located at the scene edge are focused. In Fig. 10(g), the performance of the scene edge targets reconstructed by the spectral IAA method is improved. However, the three buildings have not been distinguished. In Fig. 10(h), the imaging resolution of the three buildings becomes better using sparse Bayesian method. However, the noise amplification phenomenon appears obviously. In Fig. 10(l)–(n), the imaging performance of the IAA method, the IAA-RR method, and the DE-PIAA method are similar. They can not only distinguish three buildings but also presents superior imaging performance for the scene edge target. However, the operational complexity of the DE-PIAA method is much lower. In addition, based on the data-extrapolation process, the reconstruction performance of the DE-PIAA method in Fig. 10(n) is better than the PIAA method in Fig. 10(k).

3) Reconstruction Evaluation: For the scene edge targets as shown by the red rectangles in Fig. 10(n), we adopt image correlation coefficients to evaluate its reconstruction performance [41], [42]. Based on the extrapolated complete echo data, the correlation coefficients between the reconstructed targets and the referenced targets are listed in Table III.

In Table III, it is seen that the image correlation coefficients of the edge targets are improved for the left and right parts based on the proposed method. In which, the reconstructed results of the LSTSVD method and Tikhonov method are worse than the

other methods. The imaging result of the spectral IAA method is improved, and it is similar to the sparse method. However, their imaging performance is still limited. Based on the extrapolated complete echo data, the reconstructed performance among the traditional IAA method, the IAA-RR method, and the proposed DE-PIAA method is similar.

B. Real Incomplete Data

1) Experimental Conditions and Echo Data: In this section, the real incomplete data are applied to verify the reconstruction performance of the proposed method. In Fig. 11(a), the radar scans the waterway and the ground. The echo data are shown in Fig. 11(b). It is seen that two boats in the waterway, as shown in the red rectangle, can not be distinguished because of its coarse angular resolution. Meanwhile, the echo data of the scene edge targets are incomplete.

2) Reconstructed Target Comparison: We first obtain complete data using the data extrapolation process. The extrapolated complete echo data are shown in Fig. 12. Then, the targets are reconstructed according to different super-resolution methods, as shown in Fig. 13.

In Fig. 13, it is seen that the reconstructed results based on the extrapolated complete data are better than the incomplete data. In Fig. 13(a)–(b), the angular resolutions of these methods are improved, but the imaging results suffer from high side lobes. In Fig. 13(c), the reconstructed targets based on the spectral IAA method appear undesirable displacement. In Fig. 13(d), using the sparse Bayesian method, the false targets appear because of the noise amplification. In Fig. 13(i)–(k), the two boats in the waterway are distinguished, but the main lobe of the scene edge targets is widened.

In addition, to some extent, the imaging results are improved based on the extrapolated complete echo data. In Fig. 13(e) and (f), it is seen that the imaging results of the scene edge targets are focused. As shown in Fig. 13(g), the reconstructed scene edge based on the spectral IAA method presents lower false targets. In Fig. 13(h), the sparse Bayesian method presents enhanced angular resolution. In Fig. 13(l)–(n), the two boats in the scene center are distinguished. Meanwhile, based on the extrapolated complete echo data, the main lobes of the scene edge targets become narrow. The operational complexity of the DE-PIAA method is much less than the IAA-RR method and the IAA method.

VI. Conclusion

In this article, a DE-PIAA is proposed to fast reconstruct the targets for RAR. The proposed method first adopts the repaired steering matrix to remedy the model error. Then, the AR model is used to extrapolate the missed half beam data caused by beam scanning. Finally, the PIAA is proposed to fast reconstruct the targets. The simulated and experimental results demonstrated that the proposed DE-PIAA method can provide high-quality radar imagery for the whole observation sector with less operational complexity.

References

[1] M. I. Skolnik, *Introduction to Radar Systems*. New York, NY, USA: McGraw Hill, 1980.

[2] Y. Zhang *et al.*, "Airborne forward-looking radar super-resolution imaging using iterative adaptive approach," *IEEE J. Sel. Top. Appl. Earth Observ. Remote Sens.*, vol. 12, no. 7, pp. 2044–2054, Jul. 2019.

[3] Y. Huang, Y. Zha, Y. Zhang, Y. Wang, and J. Yang, "Real-beam scanning radar angular super-resolution via sparse deconvolution," in *Proc. IEEE Geosci. Remote Sens. Symp.*, 2014, pp. 3081–3084.

[4] W. Li, J. Yang, and Y. Huang, "Keystone transform-based space-variant range migration correction for airborne forward-looking scanning radar," *Electron. Lett.*, vol. 48, no. 2, pp. 121–122, 2012.

[5] K. Tan, W. Li, J. Pei, Y. Huang, and J. Yang, "An I/Q-channel modeling maximum likelihood super-resolution imaging method for forward-looking scanning radar," *IEEE Geosci. Remote Sens. Lett.*, vol. 15, no. 6, pp. 863–867, Jun. 2018.

[6] Y. Wu, Y. Zhang, Y. Zhang, Y. Huang, and J. Yang, "TSVD with least squares optimization for scanning radar angular super-resolution," in *Proc. IEEE Radar Conf.*, 2017, pp. 1450–1454.

[7] S. Tomei, A. Bacci, E. Giusti, M. Martorella, and F. Berizzi, "Compressive sensing-based inverse synthetic radar imaging imaging from incomplete data," *IET Radar, Sonar Navigation*, vol. 10, no. 2, pp. 386–397, 2016.

[8] J. Salzman, D. Akamine, R. Lefevre, and J. C. Kirk, "Interrupted synthetic aperture radar (SAR)," *IEEE Aerosp. Electron. Syst. Mag.*, vol. 17, no. 5, pp. 33–39, Jun. 2002.

[9] X. Bai, F. Zhou, M. Xing, and Z. Bao, "High-resolution radar imaging of air targets from sparse azimuth data," *IEEE Trans. Aerosp. Electron. Syst.*, vol. 48, no. 2, pp. 1643–1655, Apr. 2012.

[10] F.-G. Yan, B. Cao, J.-J. Rong, Y. Shen, and M. Jin, "Spatial aliasing for efficient direction-of-arrival estimation based on steering vector reconstruction," *EURASIP J. Adv. Signal Process.*, vol. 2016, no. 1, pp. 1–8, 2016.

[11] Y. Huang, Y. Zha, Y. Wang, and J. Yang, "Forward looking radar imaging by truncated singular value decomposition and its application for adverse weather aircraft landing," *Sensors*, vol. 15, no. 6, pp. 14 397–14 414, 2015.

[12] Y. Zhang, W. Li, Y. Zhang, Y. Huang, and J. Yang, "A fast iterative adaptive approach for scanning radar angular superresolution," *IEEE J. Sel. Top. Appl. Earth Observ. Remote Sens.*, vol. 8, no. 11, pp. 5336–5345, Nov. 2015.

[13] Y. Zhang, X. Tuo, Y. Huang, and J. Yang, "A TV forward-looking super-resolution imaging method based on TSVD strategy for scanning radar," *IEEE Trans. Geosci. Remote Sens.*, vol. 58, no. 7, pp. 4517–4528, Jul. 2020.

[14] Q. Zhang *et al.*, "TV-sparse super-resolution method for radar forward-looking imaging," *IEEE Trans. Geosci. Remote Sens.*, vol. 58, no. 9, pp. 6534–6549, Sep. 2020.

[15] J. Guan, J. Yang, Y. Huang, and W. Li, "Maximum a posteriori-based angular superresolution for scanning radar imaging," *IEEE Trans. Aerosp. Electron. Syst.*, vol. 50, no. 3, pp. 2389–2398, Jul. 2014.

[16] D. Zrnic and R. Doviak, "Effective antenna pattern of scanning radars," *IEEE Trans. Aerosp. Electron. Syst.*, no. 5, pp. 551–555, Sep. 1976.

[17] M. Heron, E. Gill, and A. Prytz, "An investigation of double-peaked HF radar spectra via a convolution/de-convolution algorithm," in *Proc. IEEE OCEANS -MTS/IEEE Kobe Techno-Ocean.*, 2008, pp. 1–5.

[18] Y. Zhang, Y. Huang, Y. Zha, and J. Yang, "Sparse maximuma posterior algorithm for high angular resolution of scanning radar," in *Proc. IEEE Int. Geosci. Remote Sens. Symp.*, 2015, pp. 3259–3262.

[19] Y. Zhang, Y. Zhang, Y. Huang, and J. Yang, "A sparse Bayesian approach for forward-looking superresolution radar imaging," *Sensors*, vol. 17, no. 6, 2017, Art. 1653.

[20] M. van der Baan, "Bandwidth enhancement: Inverse Q filtering or time-varying wiener deconvolution?," *Geophysics*, vol. 77, no. 4, pp. V 133-V142, 2012.

[21] J. L. Álvarez-Pérez, S. J. Marshall, and K. Gregson, "Resolution improvement of ERS scatterometer data over land by wiener filtering," *Remote Sens. Environ.*, vol. 71, no. 3, pp. 261–271, 2000.

[22] Y. Zhang, Y. Zhang, W. Li, Y. Huang, and J. Yang, "Super-resolution surface mapping for scanning radar: Inverse filtering based on the fast iterative adaptive approach," *IEEE Trans. Geosci. Remote Sens.*, vol. 56, no. 1, pp. 127–144, Jan. 2018.

[23] Y. Zhang, A. Jakobsson, Y. Zhang, Y. Huang, and J. Yang, "Wideband sparse reconstruction for scanning radar," *IEEE Trans. Geosci. Remote Sens.*, vol. 56, no. 10, pp. 6055–6068, Oct. 2018.

[24] P. Stoica, J. Li, J. Ling, and Y. Cheng, "Missing data recovery via a nonparametric iterative adaptive approach," in *Proc. IEEE Int. Conf. Acoust., Speech Signal Process.*, 2009, pp. 3369–3372.
[25] Y. Wang, P. Stoica, J. Li, and T. L. Marzetta, "Nonparametric spectral analysis with missing data via the EM algorithm," *Digit. Signal Process.*, vol. 15, no. 2, pp. 191–206, 2005.
[26] H. Chen *et al.*, "Cross-range resolution enhancement for DBS imaging in a scan mode using aperture-extrapolated sparse representation," *IEEE Geosci. Remote Sens. Lett.*, vol. 14, no. 9, pp. 1459–1463, Sep. 2017.
[27] B.-L. Cho and S.-G. Sun, "Cross-range resolution improvement in forward-looking imaging radar using autoregressive model-based data extrapolation," *IET Radar, Sonar Navigation*, vol. 9, no. 8, pp. 933–941, 2015.
[28] J. Rong, Y. Wang, and T. Han, "Iterative optimization-based ISAR imaging with sparse aperture and its application in interferometric ISAR imaging," *IEEE Sensors J.*, vol. 19, no. 19, pp. 8681–8693, Oct. 2019.
[29] D. López, L. Oehlberg, C. Doger, and T. Isenberg, "Towards an understanding of mobile touch navigation in a stereoscopic viewing environment for 3D data exploration," *IEEE Trans. Vis. Comput. Graph.*, vol. 22, no. 5, pp. 1616–1629, May 2016.
[30] P. Wang, F. Dai, M. Pan, L. Du, and H. Liu, "Radar HRRP target recognition in frequency domain based on autoregressive model," in *Proc. IEEE RadarCon*, 2011, pp. 714–717.
[31] Y. Zhang, Q. Zhang, Y. Zhang, J. Pei, Y. Huang, and J. Yang, "Fast split Bregman based deconvolution algorithm for airborne radar imaging," *Remote Sens.*, vol. 12, no. 11, 2020, Art. no. 1747.
[32] Y. Kang, Y. Zhang, D. Mao, X. Tuo, Y. Zhang, and Y. Huang, "Super-resolution doppler beam sharpening based on online Tikhonov regularization," in *Proc. 6th Asia-Pacific Conf. Synthetic Aperture Radar*., 2019, pp. 1–4.
[33] K. Ito and B. Jin, *Inverse Problems: Tikhonov Theory and Algorithms*. Singapore: World Scientific, 2015.
[34] T. Yardibi, J. Li, P. Stoica, M. Xue, and A. B. Baggeroer, "Source localization and sensing: A nonparametric iterative adaptive approach based on weighted least squares," *IEEE Trans. Aerosp. Electron. Syst.*, vol. 46, no. 1, pp. 425–443, Jan. 2010.
[35] Y. Zhang, Y. Zhang, W. Li, Y. Huang, and J. Yang, "Angular superresolution for real beam radar with iterative adaptive approach," in *Proc. IEEE Int. Geosci. Remote Sens. Symp.*, 2013, pp. 3100–3103.
[36] Y. Zhang, A. Jakobsson, and J. Yang, "Range-recursive IAA for scanning radar angular super-resolution," *IEEE Geosci. Remote Sens. Lett.*, vol. 14, no. 10, pp. 1675–1679, Oct. 2017.
[37] M. Wu, B. He, and J.-H. She, "A fast LDL-factorization approach for large sparse positive definite system and its application to one-to-one marketing optimization computation," *Int. J. Autom. Comput.*, vol. 4, no. 1, pp. 88–94, 2007.
[38] Y. Zhang, Y. Zhang, Y. Huang, W. Li, and J. Yang, "Angular superresolution for scanning radar with improved regularized iterative adaptive approach," *IEEE Geosci. Remote Sens. Lett.*, vol. 13, no. 6, pp. 846–850, Jun. 2016.
[39] G.-O. Glentis and A. Jakobsson, "Efficient implementation of iterative adaptive approach spectral estimation techniques," *IEEE Trans. Signal Process.*, vol. 59, no. 9, pp. 4154–4167, Sep. 2011.
[40] M. Wax and T. Kailath, "Efficient inversion of Toeplitz-block Toeplitz matrix," *IEEE Trans. Acoust., Speech, Signal Process.*, vol. 31, no. 5, pp. 1218–1221, Oct. 1983.
[41] K. Yen, E. K. Yen, and R. G. Johnston, "Interpretation of the correlation coefficient: a basic review," *J. Diagnostic Med. Sonography*, vol. 6, no. 1, pp. 35–39, 1990.
[42] M. Bornert *et al.*, "Assessment of digital image correlation measurement errors: Methodology and results," *Exp. Mechanics*, vol. 49, no. 3, pp. 353–370, 2009.

Deqing Mao (Student Member, IEEE) received the B.S. degree from the School of Electronic Engineering, Chengdu University of Information Technology, Chengdu, China, in 2010. He is currently working toward the Ph.D. degree with the School of Information and Communication Engineering, University of Electronic Science and Technology of China (UESTC), Chengdu, China.

His research interests include radar signal processing and inverse problem in radar imaging.

Yongchao Zhang (Member, IEEE) received the B.S. degree in electronic information engineering from Hainan University, Haikou, China, in 2011, the Ph.D. degree from the School of Information and Communication Engineering (SICE), University of Electronic Science and Technology of China (UESTC), Chengdu, China, in 2018.

From 2016 to 2017, he was a Visiting Student with the Lund University, Lund, Sweden. He is currently an Associate Research Fellow with the SICE, UESTC. His research interests include array signal processing and inverse problem in radar applications.

Yin Zhang (Member, IEEE) received the B.S. and Ph.D. degrees in electronic information engineering from the University of Electronic Science and Technology of China (UESTC), Chengdu, China, in 2008 and 2016, respectively.

From 2015 to 2016, he was a Visiting Student with the University of Delaware, Newark, DE, USA. Currently, he is an Associate Research Fellow with the School of Information and Communication Engineering, UESTC. His research interests include radar imaging and signal processing in related radar applications.

Weibo Huo (Member, IEEE) received the B.S. degree from the School of Science, Shandong Jianzhu University, Jinan, China, in 2010 and the Ph.D. degree from the School of Information and Communication Engineering, University of Electronic Science and Technology of China, Chengdu, China, in 2019.

His research interests include radar signal processing, radar target detection, and sea clutter modeling and simulation.

Jifang Pei (Member, IEEE) received the B.S. degree from the College of Information Engineering, Xiangtan University, Hunan, China, in 2010, the M.S. degree from the School of Electronic Engineering, University of Electronic Science and Technology of China (UESTC), Chengdu, China, in 2013, and the Ph.D. degree from the School of Information and Communication Engineering, UESTC, Chengdu, China, in 2018.

From 2016 to 2017, he was a joint Ph.D. Student with the Department of Electrical and Computer Engineering, National University of Singapore, Singapore. He is currently an Associate Research Fellow with the Department of Information and Communication Engineering, UESTC. His research interests include radar target recognition, radar signal processing, and machine learning.

Yulin Huang (Senior Member, IEEE) received the B.S. and Ph.D. degrees in electronic engineering from the University of Electronic Science and Technology of China (UESTC), Chengdu, China, in 2002, and 2008, respectively.

From 2013 to 2014, he was a Visiting Researcher with the University of Houston, Houston, TX, USA. Since 2016, he has been a Professor with the School of Information and Communication Engineering, UESTC. He has authored more than 80 journal and conference papers. His research interests include synthetic aperture radar, target detection and recognition, artificial intelligence, and machine Learning.

Dr. Huan is a member of the IEEE Aerospace and Electronic Systems Society.